THE MICROFLUIDIC PROBE (MFP) is a noncontact technology that applies the concept of hydrodynamic flow confinement (HFC) within a small gap to eliminate the need for closed microfluidic conduits and, therefore, overcome the conventional closed-system microfluidic limitation. Since its invention, the concept has experienced continuing advancement with several applications, ranging from manipulating mammalian cells and printing protein arrays to performing microfabrication.

One of the recent developments of the MFP technology is the microfluidic quadrupole (MQ)—a microfluidic analogy of the electrostatic quadrupoles—that is capable of generating a stagnation point (SP) and floating concentration gradients. These distinct features combined with the open-channel concept make the MFP and MQ potentially suitable tools for studying cell dynamics or diagnostic cell trapping and manipulation (using the SP).
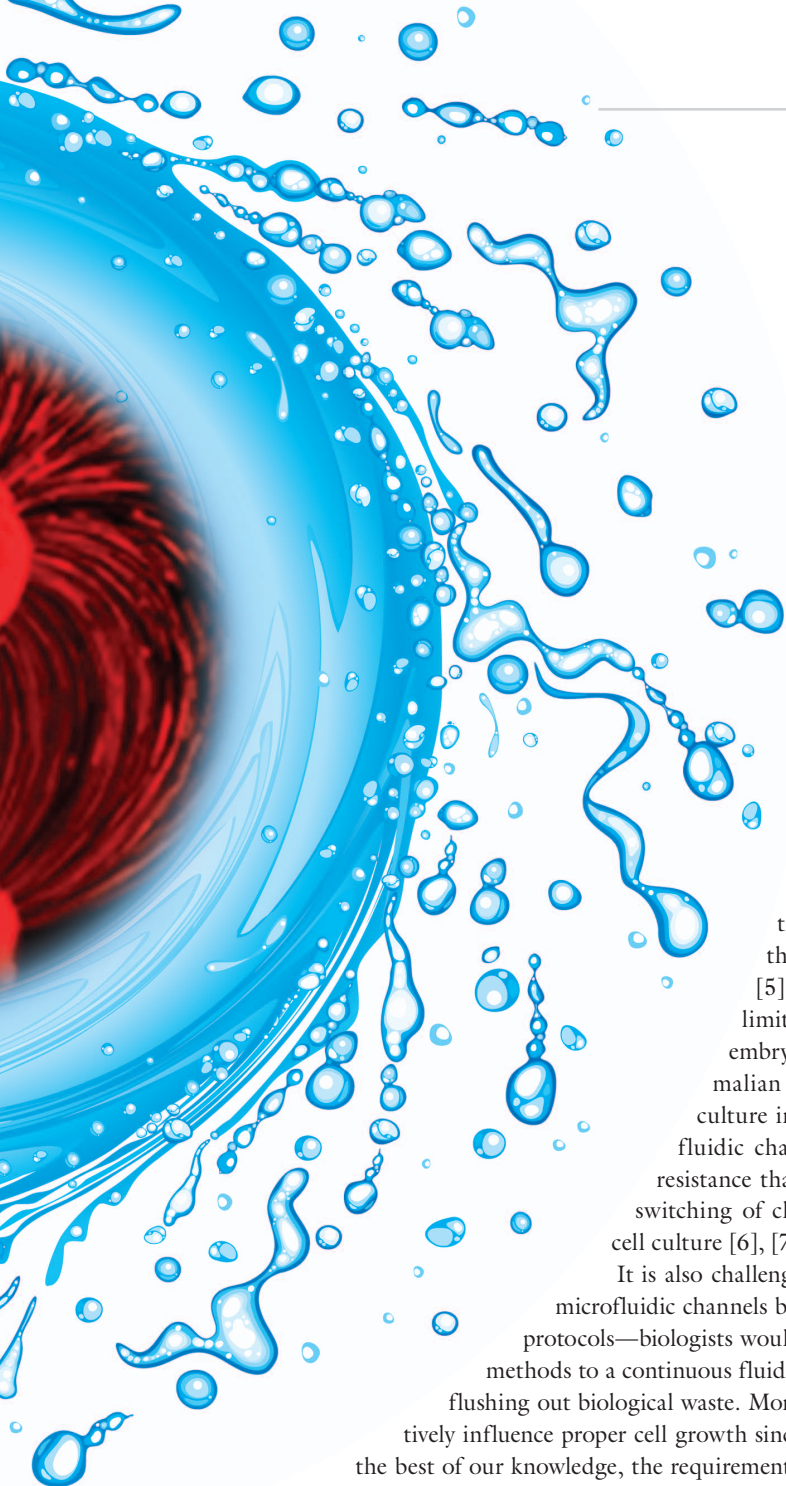
Microfluidic Probes and Quadrupoles

A new era of open microfluidics.

AYOOLA T. BRIMMO AND MOHAMMAD A. QASAIMEH
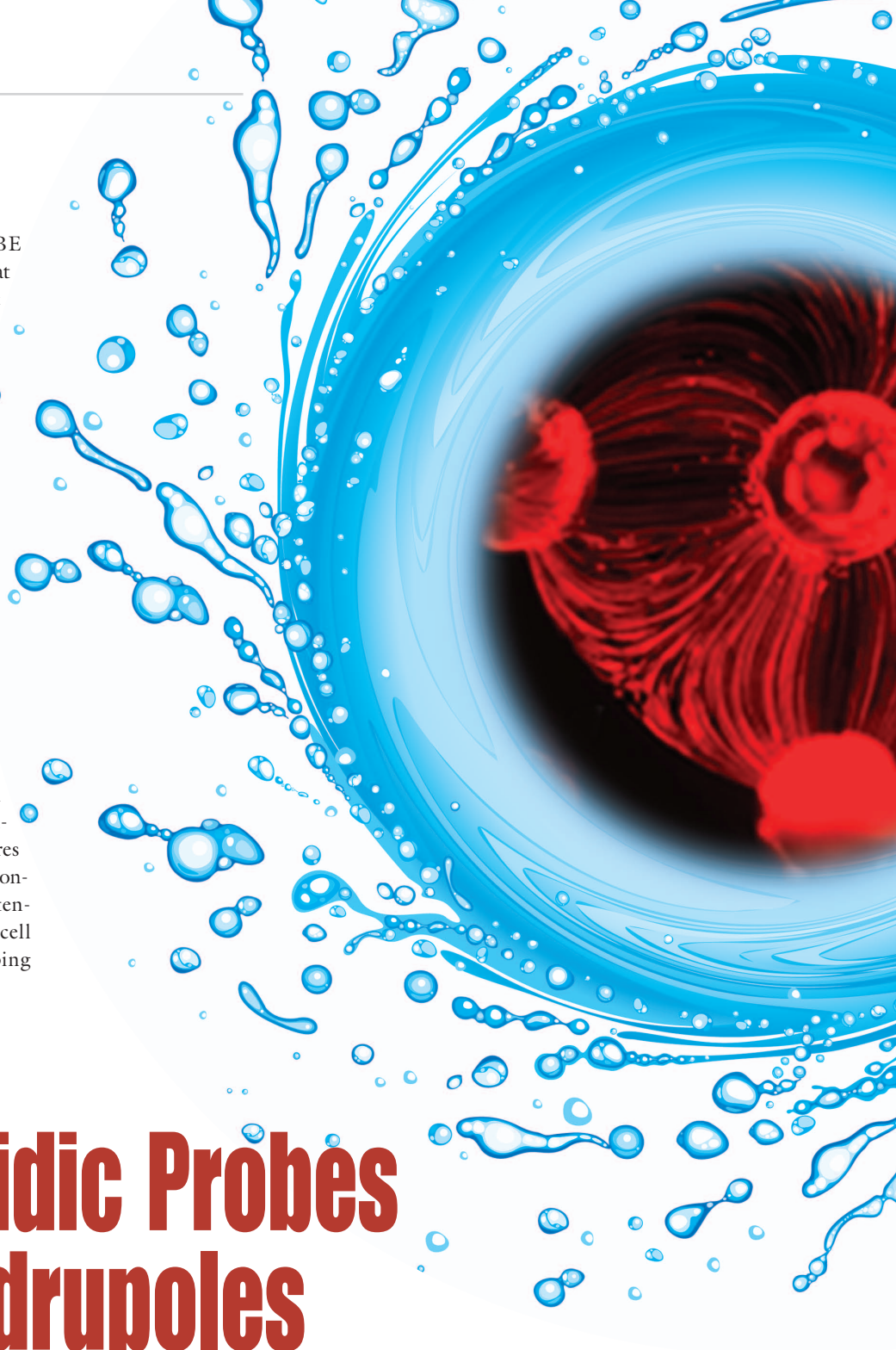
MFP TECHNOLOGY

Microfluidics is defined as the study and manipulation of fluids at the micrometer scale, where fluid flow is laminar, predictable, and controllable [1], [2]. Conventional microfluidic devices [Figure 1(a)] are typically composed of a network of channels with lengths ranging from a few millimeters to a few centimeters and heights ranging from a few micrometers to a few tens of micrometers. In chemical and biomedical analyses, dealing with fluids and devices at this scale comes with several advantages because these methods require substantially lower sample sizes (ranging from a few microliters to a few milliliters, depending on the application) and a shorter experiment-to-result time (within a few seconds to a few minutes, depending on the experiment), which reduces the experimentations costs [3]–[5]. However, the small cross-sections of microfluidic channels limit the range of biological samples that can be processed—most embryo samples and tissue slices are too large, and sensitive mammalian cells, like primary neurons and stem cells, are difficult to culture in channels of such scale. In addition, the typical long microfluidic channel with a small cross-sectional area generates high flow resistance that can cause an elevation of applied shear stresses, limit quick switching of chemicals, and introduce difficulty for a uniform in-channel cell culture [6], [7].

It is also challenging to perform a successful long-term mammalian culture in microfluidic channels because this would require the development of new cell culture protocols—biologists would need to modify conventional petri dish and microtiter plate methods to a continuous fluid flow setup for replenishing the cell culture with nutrition and flushing out biological waste. Moreover, a long-term culture with continuous flows could negatively influence proper cell growth since cell secretion could be washed away during the process. To the best of our knowledge, the requirement of developing new cell culture protocols stands as one of the main barriers to widespread applications of microfluidic technologies in biology and medicine. Consequently, the open-channel design of the MFP, which retains the advantages of the conventional microfluidic techniques while overcoming the closed-channel flow limitations, was introduced to solve these challenges [8]–[10]. With the MFP, cell culture is decoupled from the microfluidic operation, and long-term cell cultures can be performed by conventional protocols in dishes with the microfluidic operation introduced onto the cell culture at the time of the experiment [Figure 1(b)]. Since the first development of the MFP in 2005, several other open-channel microfluidic devices have also been reported [9], [11], [12].

The conventional MFP is designed with a mesa that possesses two apertures (fluidic ports): one for injecting chemicals and the other for aspiration. The mesa is immersed into the liquid, i.e., the cell culture medium when used with a cell culture, and brought in close proximity and parallel to the bottom substrate (the cell culture dish) [Figure 1(c)]. By concurrently injecting and aspirating liquid in and out of the medium, a flow pattern is created [Figure 1(d) and (e)], and, by varying flow rates, this flow pattern can be adjusted to suite specific sample manipulation requirements.

The main functionalities of the MFP are greatly dependent on the HFC of the underlying flow structure. To achieve hydrodynamic confinement, two requirements need to be satisfied: 1) the gap between the MFP mesa and the bottom
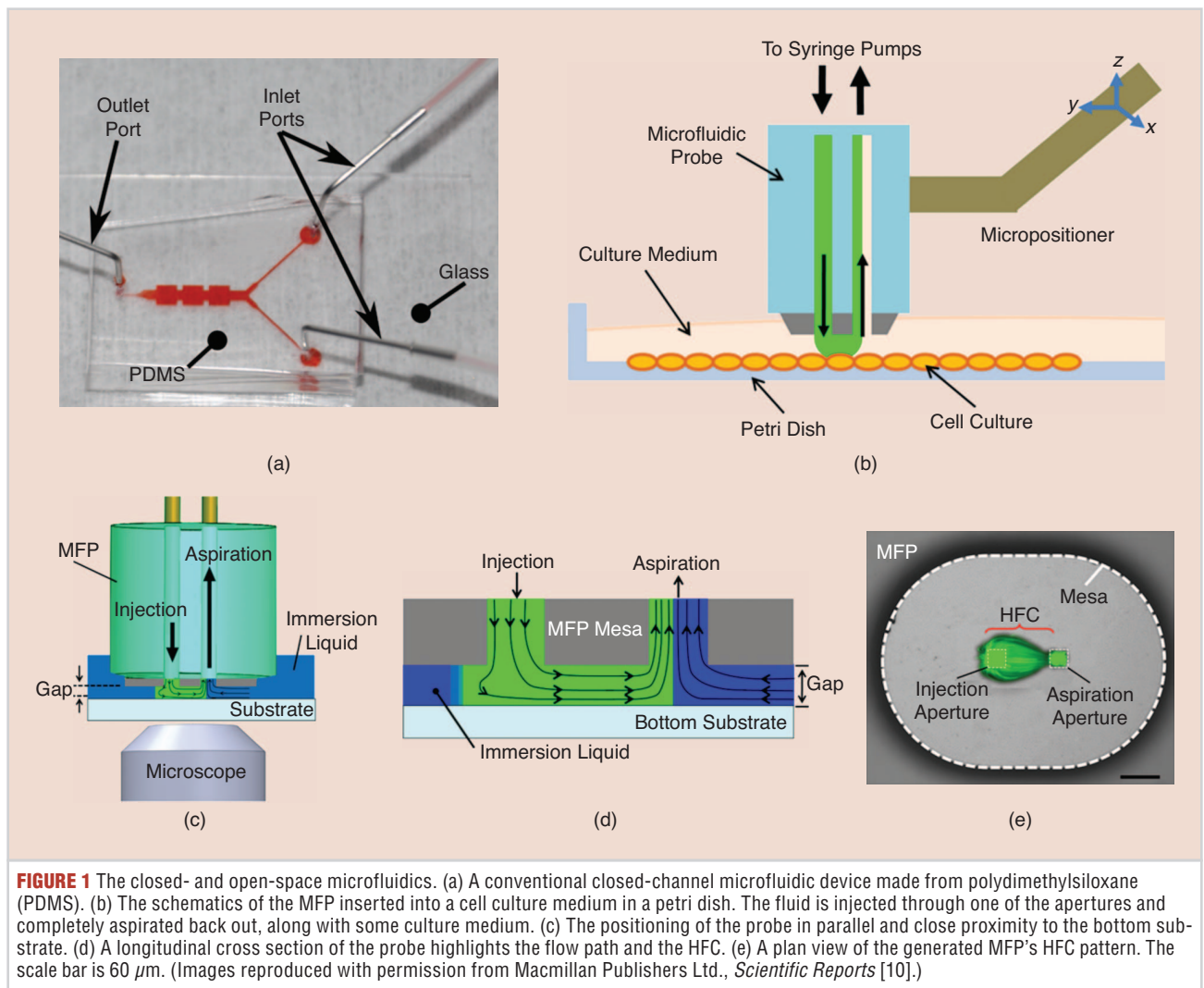
FIGURE 1 The closed- and open-space microfluidics. (a) A conventional closed-channel microfluidic device made from polydimethylsiloxane (PDMS). (b) The schematics of the MFP inserted into a cell culture medium in a petri dish. The fluid is injected through one of the apertures and completely aspirated back out, along with some culture medium. (c) The positioning of the probe in parallel and close proximity to the bottom substrate. (d) A longitudinal cross section of the probe highlights the flow path and the HFC. (e) A plan view of the generated MFP's HFC pattern. The scale bar is 60 μm. (Images reproduced with permission from Macmillan Publishers Ltd., *Scientific Reports* [10].)

substrate needs to be smaller than a certain threshold value that depends on the apertures size, aperture-to-aperture spacing, and injection-aspiration flow rates, and 2) the aspiration-injection flow ratio (Q_{asp}/Q_{inj}) needs to be higher than a certain threshold value that depends on the gap, apertures size, and spacing between them. If the MFP-substrate gap is larger than the confinement threshold value or if the Q_{asp}/Q_{inj} is smaller than the confinement threshold value, then injected fluids will partially leak out to the immersion liquid. In contrast, in the hydrodynamic confined flow regime, all injected chemicals get recaptured by the aspiration flow along with some partial withdrawal of the immersion liquid. Descriptions of the MFP operation [13], fabrication [14], [15], and use [16]–[18] are detailed in the literature.

A salient difference between the MFP and other microfluidic devices is the application of the microfluidic stream to a sample rather than the introduction of the sample in the microfluidic stream within a conduit (Figure 1). In addition, the MFP is mobile relative to the sample and can be utilized in a scanning mode. As such, the MFP has a large span of processing area and can be used to process samples with a high degree of flexibility.

The aforementioned characteristics of the MFP make it a good candidate for performing bioassays in a manner similar to conventional applications in petri dishes. This has led to several investigations with specific applications, including the tuning of microenvironments, surface biopatterning, and cell/tissue processing. Advancements in

this line have subsequently led to an extension of the MFP's configuration to include multiple injection and aspiration apertures and to the development of the MQ concept [19]. As the name implies, the MFP used to generate the MQ constitutes four microfluidic apertures—two apertures for injection and two apertures for aspiration—arranged in such a way that the injection and aspiration apertures are always adjacent to each other and in a configuration that permits hydrodynamic confinement of the injected fluids [Figure 2(a)–(c)]. Concurrent injection and aspiration of liquid through the corresponding MFP apertures produces a quadrupolar flow pattern as shown in the schematics of Figure 2(d) and the numerically calculated flow profiles of Figure 2(e). To achieve full hydrodynamic confinement

within the MQ, the small-gap and high aspiration/injection flow-rate ratio requirements also apply for each aperture pair. However, the MQ's flow structure is a bit more sophisticated as it is generated by the interaction of two flow pairs, and the desired interaction occurs only under certain operating conditions.

The flow field within the MQ is a planar extensional flow: a two-dimensional (2-D) flow consisting of purely extensional and compressional flow components with a zero-velocity SP formed at their junction [20] [Figure 2(d) and (e)].

Characteristically, the magnitude of the MQ's flow velocity is proportional to the distance from the SP along each component's direction [21]. In theory, since the fluid velocity approaches zero at the SP, diffusion dominates mass transport at this point. As such, when liquids with different chemical compositions are injected via each injection aperture, a floating concentration gradient can be formed at the SP and the fluidic interface [Figure 2(d)–(e)]. These features of the MQ are the basis behind its potential applications in life science and medicine.

MFP APPLICATIONS IN MEDICINE AND LIFE SCIENCE

CELL AND TISSUE PROCESSING

Sensitive cells such as primary neurons or stem cells can be cultured with conventional protocols when using the MFP. The experiment would typically start by bringing the culture dish from the incubator, placing it on the inverted microscope stage, and then introducing the MFP from the top until it is very close to the cell culture within the culture medium [Figure 1(b)]. Depending on the aperture diameter, spacing
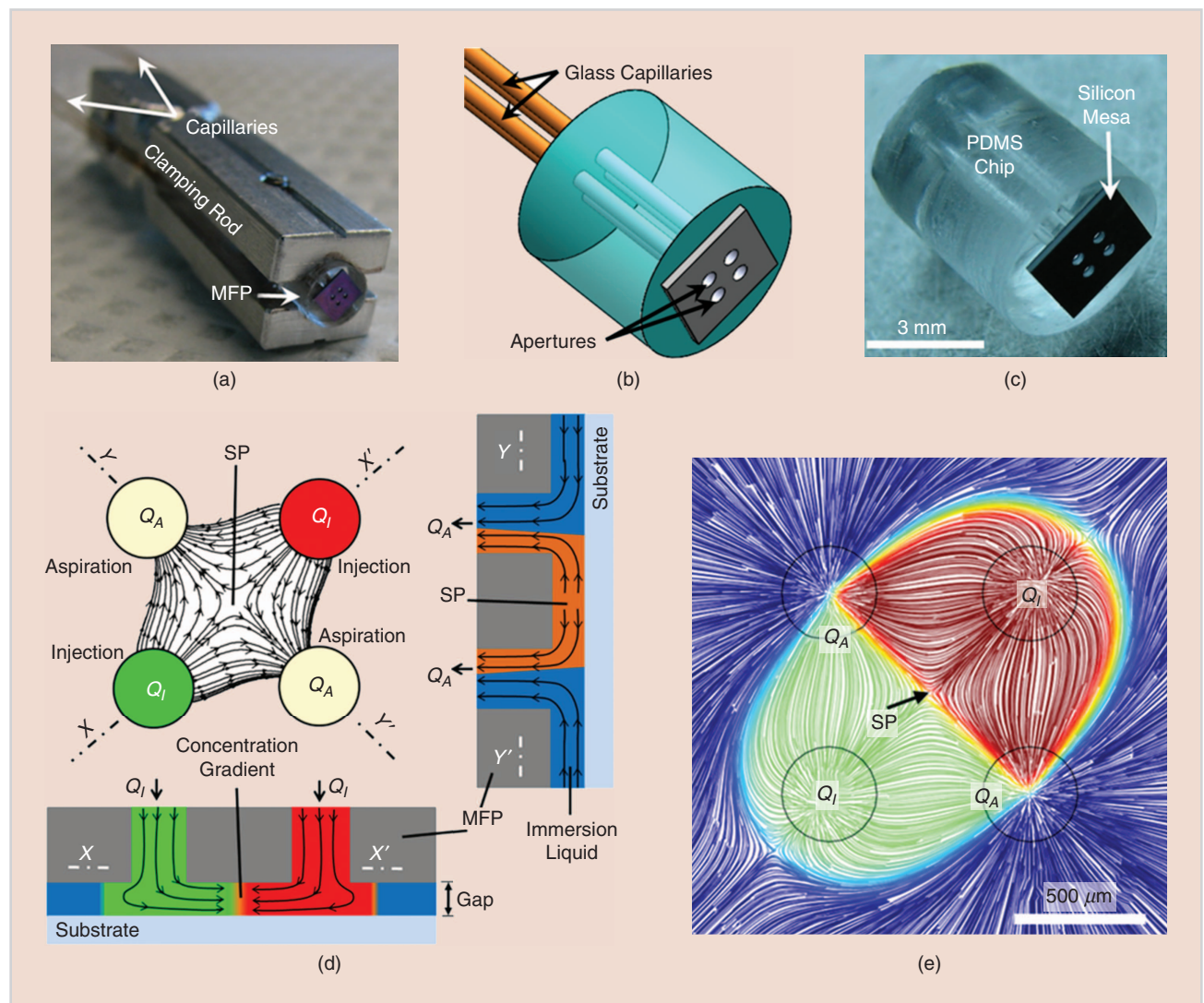
FIGURE 2 The representations of the four-aperture MFP used to generate the MQ. (a) An image of the MFP secured within the probe holder (clamping rod) and connected to capillaries. (b) A schematic of the four-aperture MFP. The apertures are arranged on the corners of an arbitrary square and supplied with +ve or −ve pressure using the glass capillaries. (c) An image of the head of the MFP with a silicon mesa and PDSM chip. (d) The schematics of the MQ concept showing the quadrupolar flow, HFC, and generated SP in the center. The insets show the XX' and YY' cross sections and highlight streamlines of the injection and aspiration flow rates. (e) The numerically calculated flow of the MQ showing the generated SP and the concentration gradient at the fluidic interface. (Images reproduced with permission from Macmillan Publishers Ltd., *Nature Communications* [19].)

(aperture-aperture), and, therefore, the area of the chemical hydrodynamic confinement, single cells may be exposed to the induced stimulus, while neighboring cells are left untouched. Moving the MFP relative to the culture or varying the scanning speed can adjust the stimulus or exposure time, respectively. The ability to move or scan the MFP also allows for unlimited serial experimentation within the same culture dish and increases the flexibility of performing several experiments in tandem. However, one limitation of this approach is its low throughput: only a few tens of cells can be studied in such experiments. This limitation can be somewhat overcome by performing serial exposures while moving the MFP.

An early demonstration of the MFP applicability with cell culture was presented by locally flushing a single cell with a solution of trypsin and detaching the cell from the culture while neighboring cells were unaffected and left adherent [22] [Figure 3(a)]. Using the same approach, single cells can be selectively detached from a culture, sucked into the aspiration aperture, and retrieved into a new location by switching the aspiration flow to injection. Another interesting application of the MFP is in handling neurons—highly branched cells with axons and dendrites [9]—that are known to be difficult to culture inside closed channels. The MFP has been proposed to locally perfuse a neuron with FluoroMyelin, a method that could be used for in vitro investigations on myelination

[23]. In a similar fashion, an axon of a hippocampal neuron was perfused with tumor necrosis factor-alpha [9], [24], and the MFP was suggested to be combined with microelectrode array technologies [25] to investigate electrical changes in neuronal networks.

The MFP is also well suited for processing large biological samples, such as tissue slices and embryos, which are relatively difficult to culture and process within closed-channel microfluidics. The MFP was used to locally perfuse tissue slices [9] that were cultured with conventional protocols like the roller-drum technique [26], [27]. A notable application was the combination of an MFP with a perfusion chamber in culturing organotypical slices for the localized microperfusion of brain tissue [14]. The setup was designed to fit on top of an inverted confocal microscope for concurrent imaging during the process. Red fluorescent dextran was locally perfused on the slice [Figure 3(b)], and the penetration within the slice's depth was recorded. The results showed that dextran penetrated to a depth of approximately 32 μm within the 70-μm-thick slice after only 12 min of perfusion with deeper penetrations at the center of the hydrodynamically confined dextran, which suggested diffusion driven mass transport.

In another application, a vertical MFP (vMFP) was developed to confine nanoliters of antibody solutions over micrometer-sized areas of tissue sections as a key step in micro-immunohistochemistry (μIHC) [28]—a method

for extracting high-quality information from tissue sections and a valuable technique for classifying cancer cells in surgical pathology [29], [30]. The footprint of the vMFP-confined liquid was observed to be comparable to areas examined using laser captured microdissection [31], [32]. The implementation of the vMFP in μIHC was reported to increase the information retrieved from very small tissue samples, minimized the volumes of antibodies, facilitated monoplex or multiplex staining of a tissue section, and offered a scanning capability. Therefore, the MFP has been suggested to work with tissues in microarray format [33], [34] and proposed to use with electrophysiology measurements to study the response of cells to drug perfusion [35]. Moreover, it has been suggested to advance the immunohistochemistry process by including the human epithelial growth factor receptor in its staining procedure [36], and it has been proposed to be used with two-photon fluorescence microscopy for deep imaging [9].

SURFACE PATTERNING
In biomedical and biological research, surfaces are often patterned with biomolecules, such as proteins and antibodies, for several applications, including immunoassays or integration with biosensors [37]. Closed-channel microfluidic use is often limited to patterning channels with a few types of biomolecules at a time. Closed channels are not flexible in terms of pattern shapes and are limited to the shape of laminar flow interfaces.

Before   After

20 μm

(a)   (b)   (c)

200 μm
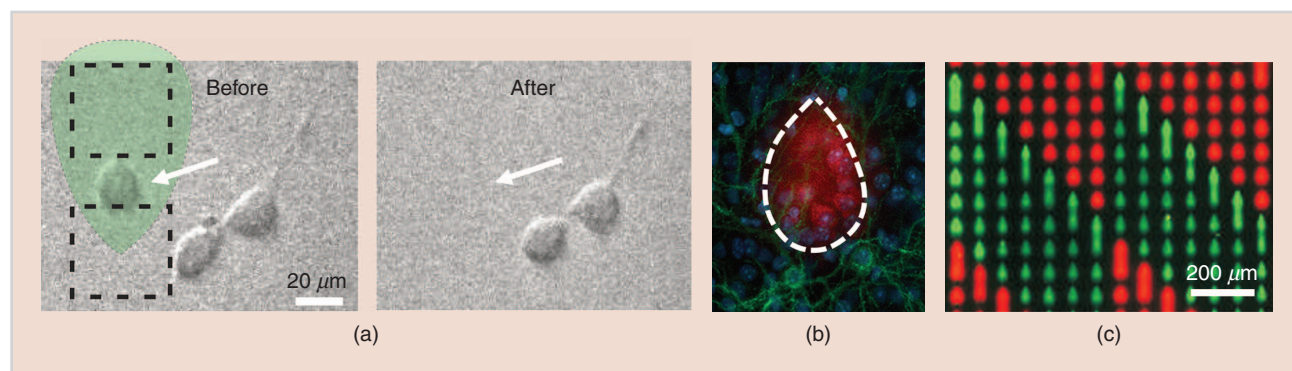
FIGURE 3 The MFP for cell, tissue, and surface processing. (a) The MFP is used to locally flush a cell with trypsin to selectively detach it while leaving surrounding cells unaltered [8]. (Image courtesy of Macmillan Publishers Ltd., Nature Materials.) (b) An organotypic brain slice is perfused locally, using an MFP, with a solution of dextran to study drug penetration at the tissue level [14]. (Image used with permission from The Royal Society of Chemistry.) (c) The patterning of a surface with high density spots of two proteins using the MFP [8]. (Images used with permission from Macmillan Publishers Ltd., *Nature Materials*.)

Traditionally, surfaces have been patterned with biomolecules using several techniques including inkjet printing and, more recently, microcontact printing [38]. While inkjet printing is the gold standard for biopatterning surfaces, the technique has several limitations such as its susceptibility to reagents drying, evaporation, and denaturation when printed on a dry surface [39].

Another notable issue is the limited patterning of spot arrays. Microcontact printing, on the other hand, is a soft lithography technique that uses soft stamps to print biomolecules on surfaces [40]. Each stamp can print one kind of pattern and protein, which limits the ease of printing several types of biomolecules on the same substrate. Since the MFP can work with any planar surface in a noncontact mode while immersed in liquid, it overcomes several challenges associated with other biopatterning techniques. The small gap between the MFP's mesa and the bottom surface enhances mass transport and biomolecule adsorption to the surface so that patterns can be produced quickly with low sample consumption using the scanning mode of the MFP.

Printing two different proteins on the same substrate constitutes the first demonstration of the MFP capabilities in biopatterning [Figure 3(c)]. Using a single run, 15,000 spot/cm^2 were achieved while maintaining the printed array immersed with the physiological liquid that prevented evaporation and protein denaturation problems [8]. Subsequently, the MFP was shown to work on both additive and subtractive modes as well as printing during scanning, which brings even more possibilities to pattern surfaces with advanced patterns that cannot be accomplished with other methods [8].

Recently, the MFP concept was developed further to include four apertures aligned on a straight line for surface patterning [41]. Two neighboring apertures were used for injecting different liquids, while the other two neighboring apertures were used for aspiration. This way, simultaneous injection and aspiration through the apertures achieved a hydrodynamically confined inner liquid enveloped within an outer confined liquid,

> **The MFP, in principle, can also be used to pattern surfaces with several types of biomolecules by a sequential switching of the injection aperture from a source to another.**

and this formed an interesting configuration that is called the *hierarchical HFC*. By optimizing injection and aspiration flow rates, the multiple layers of liquids can be selectively brought into contact with the bottom surface. Therefore, this MFP can be used to address critical aspects of microscale surface processing through minimal dilution, efficient retrieval, and fast switching of chemicals in a confined region.

The hierarchical MFP was portrayed to be applicable in removing functionalized deoxyribonucleic acid (DNA) from a surface with a sixfold increase in DNA retrieval compared to the original MFP device with only two apertures. This was achieved by injecting a solution of sodium hydroxide—using the inner HFC to denature DNA locally and remove the fluorescently labeled DNA strand from the surface. Similar techniques can be used to recover or isolate samples, such as nucleic acids or other ligands, from specific sites on microarrays or from selected adherent cells. Another application of hierarchical MFP is a simultaneous deposition of two proteins on a surface using compartmentalization of the proteins in either the inner or the outer HFC. Remarkably, the resolution of patterns created on surfaces was observed to be adjustable by varying the gap between the MFP and the bottom substrate, and in comparison to the conventional MFP technique, a threefold decrease in the consumption of chemical reagents was recorded when processing a surface using the outer HFC flow [41].

The MFP, in principle, can also be used to pattern surfaces with several types of biomolecules by a sequential switching of the injection aperture from a source to another. This procedure,

performed in a preprogrammed manner, can bring several advances to the fields of immunoassays, cell biology studies, biosensors, and tissue engineering. However, for processing large areas, one needs to make sure the MFP and the bottom substrate are perfectly aligned (in parallel to each other) to guarantee uniformity in the printing density and to avoid any physical contact between the MFP and the substrate.

One technique to solve this issue was developed by integrating a fluidic mechanism to control the distance between the MFP and the sample [18]. The concept is denoted as the floating MFP, where two additional apertures were introduced farther away from the patterning injection-aspiration apertures and used for injecting medium-to-high flow rates into the gap to cause hydrodynamic levitation of the MFP. A balance between the hydrodynamic levitation force and the MFP's other external forces defines the gap size, and this gap is maintained even when the bottom substrate is not uniform. By adapting similar techniques, large areas can easily be patterned using the MFP; however, there is a limitation in the volume of the biomolecules source as this depends on the size of the typically adapted glass syringe. As refill mechanisms are typically associated with microfluidic pumping systems, this issue is not expected to cause a major problem.

CONCEPTS AND CONFIGURATIONS OF MQS

The two-aperture MFPs can be described as a microfluidic dipole, analogous to electrostatic dipoles, where the injection aperture represents the positive charge element and the aspiration
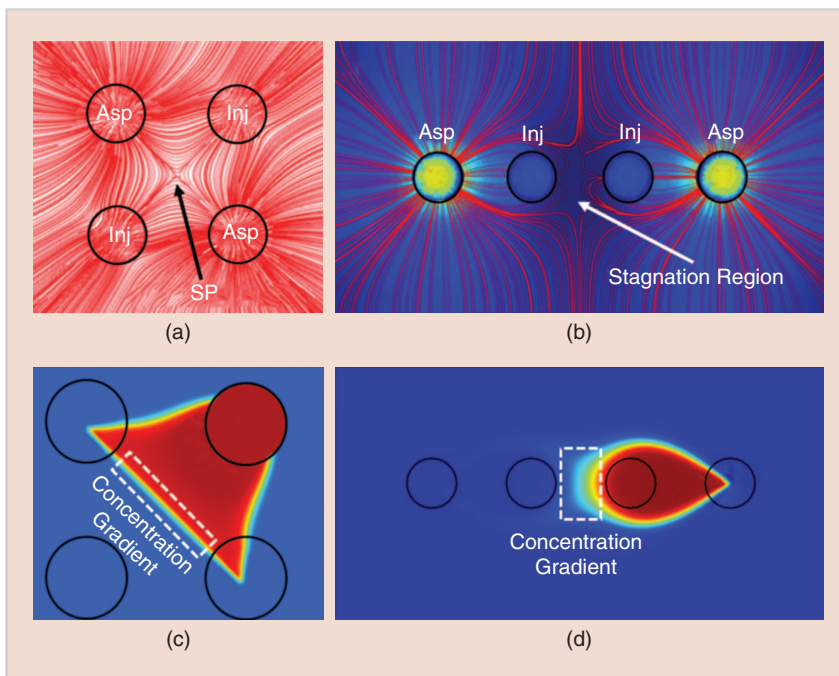
FIGURE 4 The stagnations and concentration gradients within the MQ. (a) The streaklines of the lateral MQ flow. The SP is formed at the intersection of all flows. (b) The streaklines of the linear MQ. The aspiration apertures (Asp) are positioned at the outer end of the line, and the injection apertures (Inj) are positioned at the middle. (c) A sharp concentration gradient generated by the lateral MQ. (d) A long range concentration gradient generated by the linear MQ. [(a) and (c) reproduced with permission from Macmillan Publishers Ltd., *Nature Communications* [19].]

aperture represents the negative charge element. The fact that the gap between the MFP and the substrate is significantly smaller than the MFP mesa dimensions reduces the problem to a 2-D microfluidic dipole and makes modeling the phenomena relatively easy [10]. In a similar fashion, the MQ is a 2-D fluidic analog to electrostatic quadrupoles, with two injection apertures and two aspiration apertures. Thus, an MQ is a combination of two microfluidic dipoles positioned in close proximity and formed using an MFP with four apertures, where an injection aperture is always positioned next to an aspiration aperture.

To date, there are two distinct configurations of MQs: the lateral MQ and the linear MQ. As shown in Figure 4(a), with the lateral MQ, the apertures are positioned on the corners of a virtual square, where similar (+ve or –ve) apertures are arranged diagonally. As described previously, injected chemicals meet heads-on at the center, create an SP with zero flow, and then split to each aspiration aperture. On the other

hand, in the linear MQ [Figure 4(b)], the apertures are arranged on a straight line with aspiration apertures positioned at the outer ends of the line. Due to the linear MQ's aperture configuration, each neighboring aspiration aperture also confines injected chemical and, therefore, leaves a stagnation region in-between both chemicals. Modulating the aspiration/injection flow rates ratio can control the size of this stagnation region; some preliminary results suggest that the region could be shrunk down to a point where the injected chemicals meet heads-on at the center.

In both types of MQ, chemical diffusion occurs across fluidic stagnation areas, and it interfaces and generates concentration gradients. In the lateral MQ, the diffusion occurs across the SP as well as the fluidic interface [Figure 4(a) and (c)]. With the linear MQ, the diffusion occurs across the stagnation region [Figure 4(b) and (d)]. In general, one of the injected chemicals represents the gradient source, while the other injected fluid operates

as a sink for the gradient. However, there are some differences between the gradients generated by lateral and linear MQ: the lateral MQs are much shorter and faster to establish in comparison to the gradients established within the linear MQ.

VISUALIZING THE MQ'S SP AND STAGNATION REGION

Three-dimensional multiphysics modeling and simulations confirmed the formation of an SP and a stagnation region within the lateral and linear MQs, respectively (Figure 4). Experimentally, an inverted fluorescence microscope was used to visualize the quadrupolar pattern and stagnations of the MQ flow. For the lateral MQ flows, solutions of green and red tracer beads were injected through each injection aperture, respectively, while the immersion liquid was clear deionized water. By increasing the exposure time for the acquired image through the sensitive camera connected to the microscope, streakline images for the quadrupolar flow were observed [Figure 5(a)].

Clearly, the beads carried with the flow are shown as streaklines, and the SP is observed where the lines converge and get deflected toward the aspiration apertures, leaving the SP with zero flow velocity. The used tracer beads are 2 μm in size so their diffusion is negligible. Immobilized beads [shown as dots in Figure 5(a)] sticking to the substrate were used as reference points.

To visualize the linear MQ, the immersion liquid was mixed with tracer beads while injected liquids were clear deionized water. The hydrodynamically confined injected liquids are shown in Figure 5(b) as two black spots with a tear shape, and the fluid flow is observed by the bead's streaklines following imaging after a long exposure time. In Figure 5(b), streaklines can be seen converging near the stagnation region that is observed by the immobile beads, and they get deflected toward the aspiration apertures. Immobile beads, shown as dots, are suspended within the immersion liquid in-between the injection apertures, and they do not encounter fluid flow.
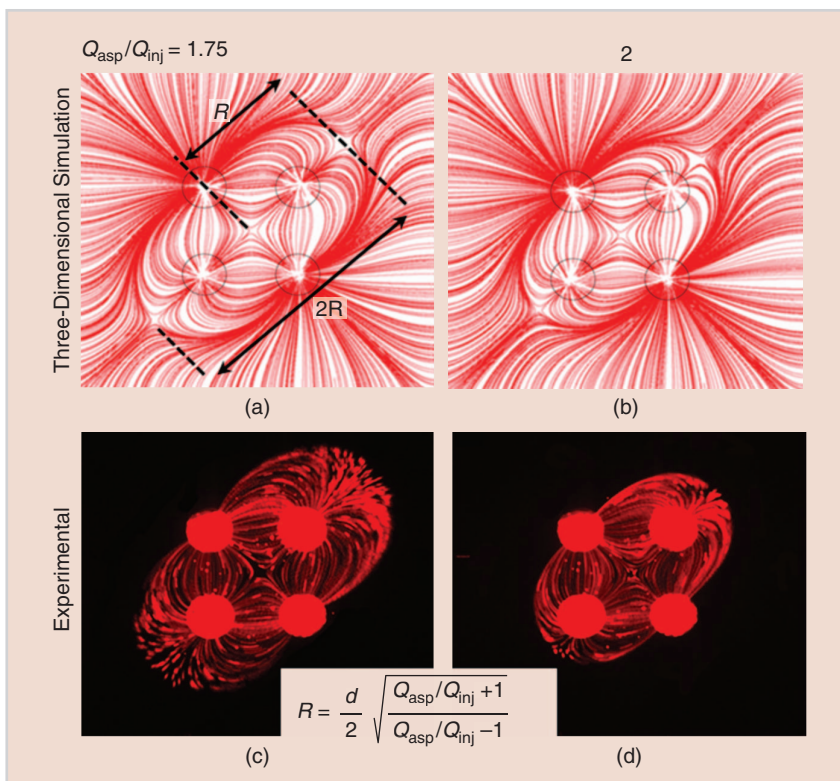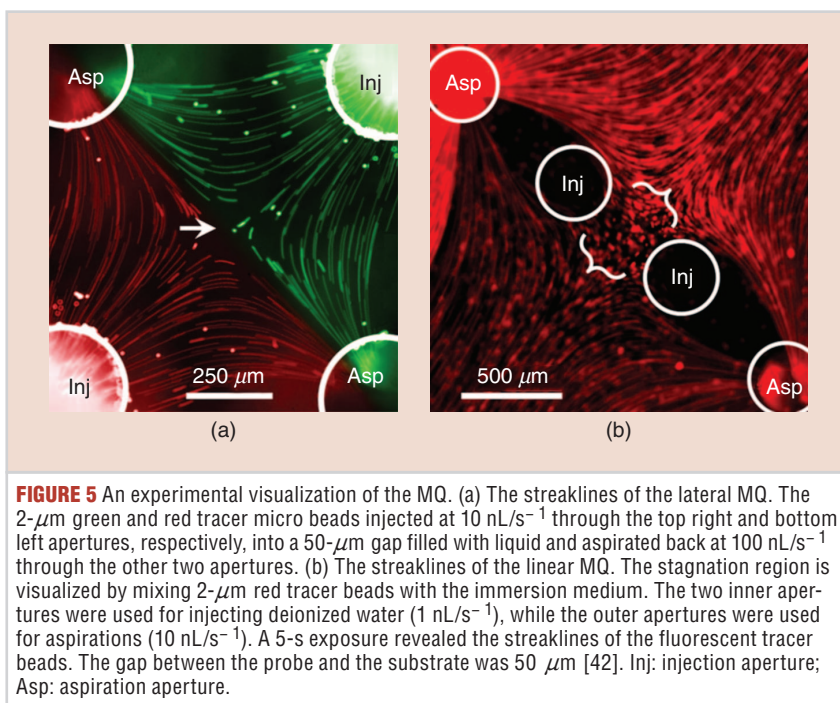
CONTROLLABLE LATERAL MQ FLOW AND SP POSITIONING

To achieve the HFC of the MQ, the aspiration flow (Q_{asp}) must be sufficiently larger than the injection flow (Q_{inj}) so that all of the injected fluid is reaspirated back. Otherwise, parts of the injected fluid leak out to the immersion flow and make it difficult to define a region that the MQ spans over. As chemicals injected into the streams may be used to process the underlying surface selectively [8], the confinement area of the MQ is of significance. Varying Q_{asp}/Q_{inj} from 1.75 to 2, numerically and experimentally deduced streamlines of the lateral MQ are presented in Figure 6, highlighting the variation in the confinement area. Measurements of the confinement radius, defined as the distance between the SP and the outermost point of zero velocity from the radial streams [Figure 6(a)] as a function of flow ratio (Q_{asp}/Q_{inj}), portray a decrement in the confinement radius R as the ratio increases.

Since the aspiration aperture captures all of the injected fluid, at a steady state, the spread of the injected fluid becomes larger as the aspiration flow rate is reduced relative to the injection flow rate. This increase in the spread continues until a certain threshold of the flow ratio is reached, and the flow structure is broken with leakage to the immersion fluid. The corresponding measured relation between the flow ratio and the confinement radius was shown to be in quantitative agreement with the analytical equations (Figure 6) formulated using the Hele-Shaw approximation (2-D Stokes flow) [19].

By changing the conventional unity aspiration and injection flow ratios (make $Q_{in1}/Q_{in2} \neq 1$ and $Q_{asp1}/Q_{asp2} \neq 1$), the MQ can be used to generate complex flow patterns. Such adjustments also serve as a tuning mechanism for the position and dynamics of the SP. In Figure 7, the red tracer beads are injected through one of the apertures and deionized water is injected through the other, while the injections (Q_{in1}/Q_{in2}) and aspirations (Q_{asp1}/Q_{asp2}) ratios are varied.

Figure 7(a) shows the symmetric flow streaklines of the MQ when the injection and aspiration flow ratios are both

FIGURE 5 An experimental visualization of the MQ. (a) The streaklines of the lateral MQ. The 2-μm green and red tracer micro beads injected at 10 nL/s^{-1} through the top right and bottom left apertures, respectively, into a 50-μm gap filled with liquid and aspirated back at 100 nL/s^{-1} through the other two apertures. (b) The streaklines of the linear MQ. The stagnation region is visualized by mixing 2-μm red tracer beads with the immersion medium. The two inner apertures were used for injecting deionized water (1 nL/s^{-1}), while the outer apertures were used for aspirations (10 nL/s^{-1}). A 5-s exposure revealed the streaklines of the fluorescent tracer beads. The gap between the probe and the substrate was 50 μm [42]. Inj: injection aperture; Asp: aspiration aperture.

$$R = \frac{d}{2}\sqrt{\frac{Q_{asp}/Q_{inj} + 1}{Q_{asp}/Q_{inj} - 1}}$$

FIGURE 6 The numerical and experimental flow confinement of the lateral MQ. (a) The numerically calculated streamlines for the MQ with $Q_{asp}/Q_{inj} = 1.75$. The confinement radius is defined as the distance between the SP and the outermost point of zero velocity from the radial streams. (b) The numerically calculated streamlines with $Q_{asp}/Q_{inj} = 2$. The spread of the flow shrinks so that the confinement radius reduces. (c) The experimentally captured images of the MQ with a flow ratio of 1.75. (d) The experimentally captured image of the MQ with a flow ratio of 2. Inset: The analytical formula for estimating the confinement radius. Each aperture size is 360 μm. (Images reproduced with permission from Macmillan Publishers Ltd., *Nature Communications* [19].)

unity. However, as shown in Figure 7(b), increasing the injection flow Q_{in2} to a value of seven times that of Q_{in1}, while leaving the aspiration flow rates identical, breaks the MQ's symmetry and moves the SP closer to Q_{in1}, along the axis connecting the injection apertures. In a similar fashion, a different flow structure can be formed by increasing Q_{in1} to a value of ten times that of Q_{in2}, [Figure 7(c)]. Figure 7(d)–(e) shows that the SP can be also moved along the axis connecting the aspiration apertures by varying the ratio of aspirations. Furthermore, more complex flow structures and 2-D movement of the SP can be achieved by simultaneously varying both injections and aspirations ratios [Figure 7(f)]. Using this dynamic response of the SP, the MQ can be potentially used to trap objects and move in a 2-D pattern.

CONCENTRATION GRADIENTS

Concentration gradients within the MQ are formed by diffusion from one of the injected fluids to the other at the flow divergence junction of the MQ (the axis connecting the aspiration apertures). As such, to generate concentration gradients, the injected fluids through each aperture are required to be of different chemical compositions. As shown in Figure 8, the injection of a fluorescein solution through one aperture and deionized water through the other was used to demonstrate the generation of concentration gradients with the lateral MQ [19]. Starting with a flow ratio of 2 [Figure 8(a)], the spread (the radius of confinement) of the injected fluorescein solution is seen to progressively reduce as the flow ratio is increased to 10 and 20 in Figure 8(b) and (c), respectively.

This is in accordance with the theory explained in the section "Controllable Lateral MQ Flow and SP Positioning." However, as demonstrated in the images inset [Figure 8(a)–(c)], in addition to varying the confinement size, the size of the concentration gradient can also be manipulated by the flow ratio.

Experiments and mathematical models were used to derive a theoretical framework, $L_g = \beta \sqrt{D/Q_{asp} + Q_{inj}}$, which can be used to precisely predict the size of the concentration gradient. L_g is the length of the produced gradient, β is a constant that depends on the spacing between the injection apertures and the MFP-to-substrate gap, and D is the diffusion coefficient of the injected solute [19].

The experiments also confirmed the uniformity of the gradient size across
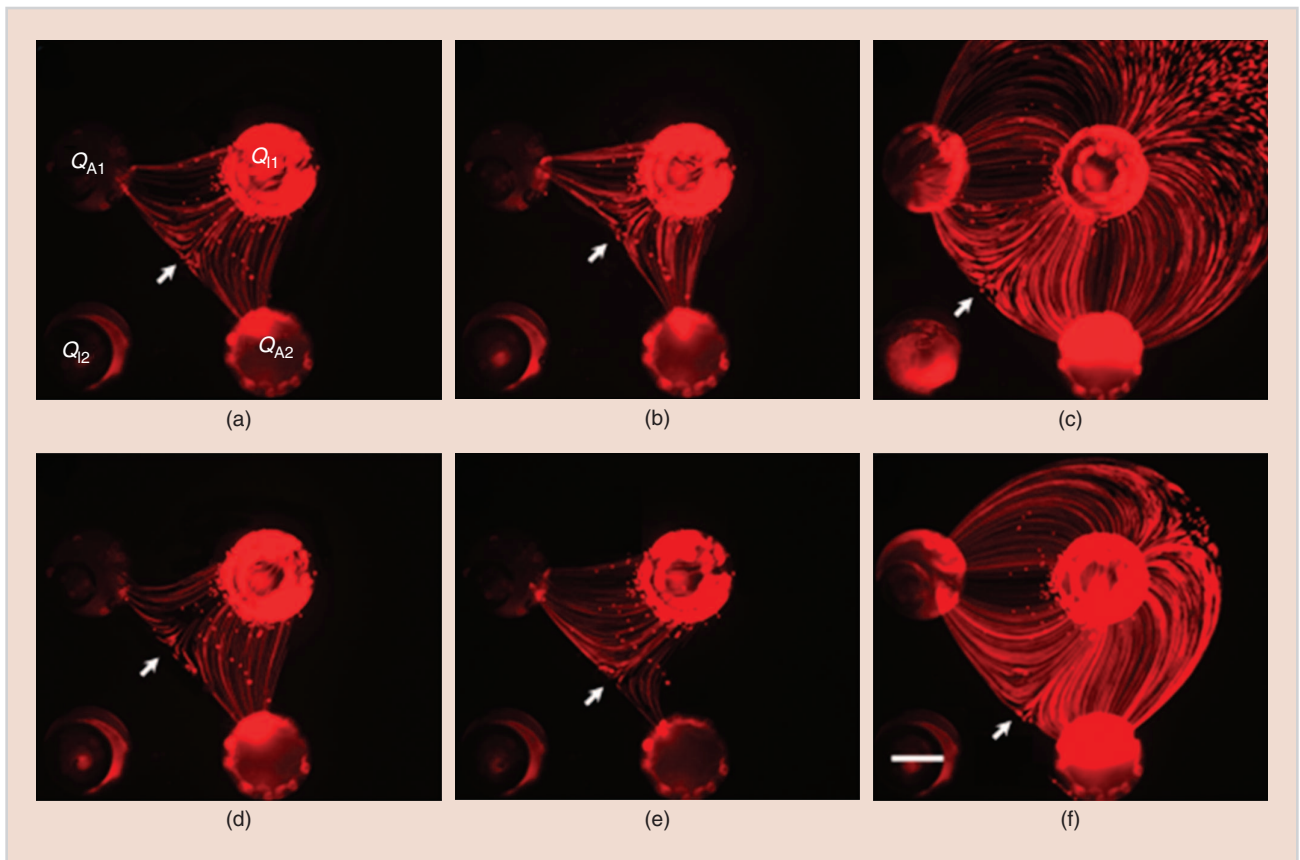
FIGURE 7 The hydrodynamic positioning of the SP within the lateral MQ. (a) The symmetric flow with $Q_{in1} = Q_{in2} = 10$ and $Q_{asp1} = Q_{asp2} = 100$. (b) The MQ with $Q_{in1} = 10$, $Q_{in2} = 70$, and $Q_{asp1} = Q_{asp2} = 100$. The symmetry is broken due to the variation in the injection flow rate. The SP is moved toward the low inlet flow aperture (Q_{in1}) along the axis connecting both injection apertures. (c) The MQ with $Q_{in1} = 100$, $Q_{in2} = 10$, and $Q_{asp1} = Q_{asp2} = 100$. The SP is moved toward the low inlet flow aperture (Q_{in2}). (d) The MQ with $Q_{in1} = Q_{in2} = 10$ and $Q_{asp1} = 150$, $Q_{asp2} = 100$. The SP is moved toward the high aspiration flow aperture (Q_{asp1}) along the axis connecting both aspiration apertures. (e) The MQ with $Q_{in1} = Q_{in2} = 10$ and $Q_{asp1} = 100$, $Q_{asp2} = 170$. The SP is moved toward the high aspiration flow aperture (Q_{asp2}). (f) The MQ with $Q_{in1} = 90$, $Q_{in2} = 10$, and $Q_{asp1} = 70$, $Q_{asp2} = 190$. Movement of the SP is in 2-D and, therefore, the MQ is of asymmetric shape. All flow units are in nL/s^{-1}. The scale bar is 200 μm.
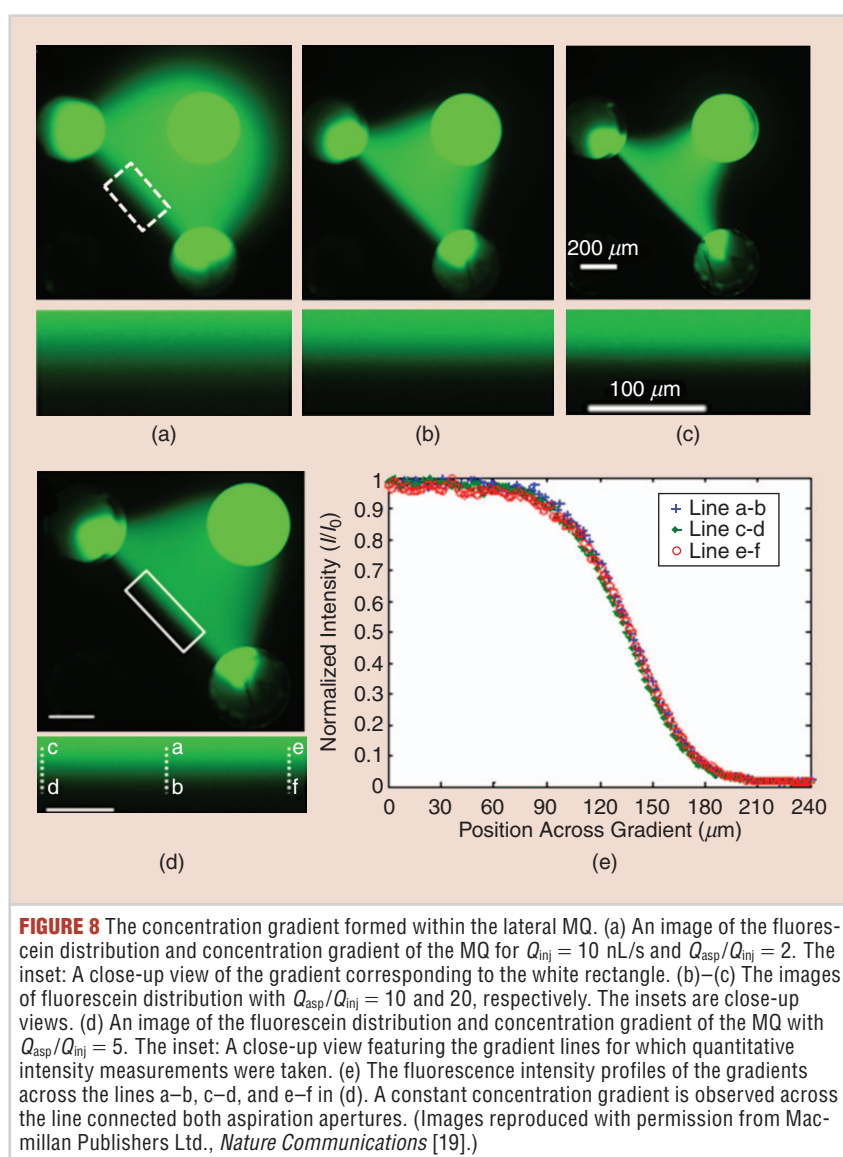
the axis joining the aspiration apertures [Figure 8(d)], which was correspondingly observed in numerically obtained results. The normalized fluorescent intensity as a function of the position across the lines a–b, c–d, and e–f, are shown in Figure 8(e), which identically matches.

Furthermore, simulations of the MQ fluid flow show that the minimum flow speed is at the SP where injected chemicals meet head on, whereas the maximum flow speed exists at the edge of the aspiration aperture. The fluids accelerate after splitting and deflecting toward each aspiration aperture until reaching maximum speed at the aspiration aperture edge. Therefore, convection dominates diffusion except at the SP. This explains the uniform gradient size across the interface, particularly when considering the strong concentric flow around the aspiration apertures that focuses the gradient stream and counter diffusive broadening of the gradient. Furthermore, transient measurements show that the gradient can be modulated rapidly, in a matter of seconds, which suggests that dynamic gradients can be readily formed by preprograming the working flow rates.

The SP movement explained in the previous section (Figure 7) also suggests the movement of the gradient hydrodynamically, as the fluidic interface will be curved toward the weaker injection aperture. The same can be achieved using the linear MQ—its hydrodynamics also allow for resizing and repositioning of the stagnation region, and, therefore, forming of the concentration gradient, by modulating Q_{asp}/Q_{inj}. By automating this flow via a code, dynamic gradients can also be generated, and this can be extended to more complex landscapes by increasing the number of apertures. This programmable concentration gradient feature of the MQ has a good potential in life science applications like reproducing cellular microenvironments [43], [44], differentiating cells, and developing organisms [45], [46]. However, it must be noted that work on this concept with the linear MQ is still under development.

FUTURE OUTLOOK

The concept of open microfluidics is still new and needs to be developed further

FIGURE 8 The concentration gradient formed within the lateral MQ. (a) An image of the fluorescein distribution and concentration gradient of the MQ for $Q_{inj} = 10$ nL/s and $Q_{asp}/Q_{inj} = 2$. The inset: A close-up view of the gradient corresponding to the white rectangle. (b)–(c) The images of fluorescein distribution with $Q_{asp}/Q_{inj} = 10$ and 20, respectively. The insets are close-up views. (d) An image of the fluorescein distribution and concentration gradient of the MQ with $Q_{asp}/Q_{inj} = 5$. The inset: A close-up view featuring the gradient lines for which quantitative intensity measurements were taken. (e) The fluorescence intensity profiles of the gradients across the lines a–b, c–d, and e–f in (d). A constant concentration gradient is observed across the line connected both aspiration apertures. (Images reproduced with permission from Macmillan Publishers Ltd., *Nature Communications* [19].)

before being used as a standard technology in biomedicine and life science [47]–[49]. Although research and development still have a key role to play before these technologies can achieve commercialization [50]–[52], a few open microfluidic systems have successfully made it to the market [53], [54]. The same applies to the concepts of the MFP [8] and the MQ [19], where more research, applications, and developments in their setup are still required. However, for substantial progress to be recorded with applications of these devices, their unique features have to be leveraged and highlighted in the future.

For the MFP, its open and mobile setting is expected to impact single cell studies and surface patterning. The MQ

is notable because of its dynamic and controllable SP, and concentration gradients, which hold promise for future applications in trapping and manipulating cells. The unique features of the MFP and MQ also usher in applications in capturing, enumerating, and characterizing biological particles and scanning over biological samples for dynamic sampling and stimulations. The open configuration of the MFPs, in general, represents a new era of open microfluidics since cell and tissue cultures are decoupled from the microfluidic processes, and microfluidics are brought to the sample instead of bringing the sample inside the microfluidic channels. These features can be simply envisioned

> ## One interesting potential future application of the MQ is in the detection of target-sequences by trapping and stretching DNA at the SP.

as bringing microfluidics to the culture dish where cell and tissue cultures are performed using conventional methods.

One interesting potential future application of the MQ is in the detection of target-sequences [55] by trapping and stretching DNA at the SP. This can be used to elucidate the fundamental understanding of the transcription of genetic information from DNA to a messenger ribonucleic acid using transcription factors [56], [57]. Another fascinating potential application is the trapping of cells at the SP for studying cell dynamics [58] and deformability [59], [60] akin to closed-chip microfluidics [61], [62] but utilizing the open nature and scanning capability of MQs. Furthermore, the MQ's generated floating concentration gradient can be used for cell chemotaxis studies, neuronal navigation, cancer cell migration, and stem cell differentiations. An early biological application of the MQ was shown in applying the floating concentration gradients to a culture of neutrophils, a type of white blood cells. While the study is still in progress, preliminary results show distinct responses and the dynamics of cells' chemotaxis when challenged with stationary versus moving gradients [63], [64].

The future we envisage for the MFP and MQ is evolving from the current form, as experimental tools, to the integrated lab-on-tip devices used commercially. However, this transformation is highly reliant on how much these devices can be used to simplify conventional processes with a high level of sensitivity, selectivity, and throughput [65], [66]. For the MFP and MQ to attain this, considerable efforts need to be made to establish integrated tools without dependence on external devices. In addition, methods of automatically moving the MFP and the MQ's

SP and concentration gradients on a preprogrammed manner can enhance their transformations to biological and clinical laboratories.

CONCLUSIONS

The emergence of the MFP and MQ in microfluidics has the potential to develop a new era in the field. However, practical applications of these technologies in biology and life science are key steps in transitioning their current laboratory forms to physical lab-on-tip tools used commercially. This article reviewed recent developments in MFP and MQ technologies and highlights their promising features. The open nature of MFP and MQ concepts are particularly interesting due to the flexibility they offer. The MFP device can be introduced into the experiment at any time and does not require users to shift from conventional biology protocols. However, a key requirement to their operation is ensuring that the devices are setup in such a way that the parallel plate-plate requirement is upheld. The parallel plate requirement presents some difficulty in setting up the experiments, as perfect alignment is difficult to attain at the micro scale. Although, some techniques have been shown to ease this process, a full automation of the process is required.

The MFP has been proven to be a good candidate for complex shape biopatterning and multiplexing because it solves the problems of protein denaturation and sample evaporation during printing. The SP of the MQ has a potential for trapping and manipulating cells (e.g., stretching DNA); however, practical applications for the SP are still yet to be demonstrated.

On the other hand, some preliminary studies have exhibited the potential of the generated concentration gradient for chemotaxis studies. The scanning capability of this generated gradient could

extend such studies to the investigation of chemotaxis within moving gradients. The open nature of the concept also makes it a good candidate for studying sensitive cells, such as primary neurons or stem cells. The resolution of the MFP, and therefore the MQ, is highly dependent on the aperture and mesa sizes, and so there is also a potential to scale the technology down to even subcellular resolutions. Although this comes at a cost of low throughput, perhaps this can open doors for MFP and MQ applications at the submicron scale.

ABOUT THE AUTHORS

Ayoola T. Brimmo (tab478@nyu.edu) is with the Engineering Division of the New York University Abu Dhabi, United Arab Emirates, and the Mechanical and Aerospace Engineering Department of the New York University Tandon School of Engineering, Brooklyn.

Mohammad A. Qasaimeh (mohammad .qasaimeh@nyu.edu) is with the Engineering Division of the New York University Abu Dhabi, United Arab Emirates, and the Mechanical and Aerospace Engineering Department of the New York University Tandon School of Engineering, Brooklyn.

REFERENCES

[1] J. Puigmartí-Luis, "Microfluidic platforms: A mainstream technology for the preparation of crystals," *Chem. Soc. Rev.*, vol. 43, no. 7, pp. 2253–2271, 2014.

[2] G. M. Whitesides, "The origins and the future of microfluidics," *Nature*, vol. 442, no. 7101, pp. 368–373, July 2006.

[3] C. Hansen and S. R. Quake, "Microfluidics in structural biology: Smaller, faster… better," *Current Opinion Structural Biol.*, vol. 13, no. 5, pp. 538–544, 2003.

[4] G. A. Cooksey, J. T. Elliott, and A. L. Plant, "Reproducibility and robustness of a real-time microfluidic cell toxicity assay," *Anal. Chem.*, vol. 83, no. 10, pp. 3890–3896, 2011.

[5] A. L. Paguirigan and D. J. Beebe, "Microfluidics meet cell biology: Bridging the gap by validation and application of microscale techniques for cell biological assays," *BioEssays*, vol. 30, no. 9, pp. 811–821, Sept. 2008.

[6] E. W. Young and D. J. Beebe, "Fundamentals of microfluidic cell culture in controlled microenvironments," *Chem. Soc. Rev.*, vol. 393, no. 3, pp. 1036–1048, Mar. 2010.

[7] G. M. Walker, H. C. Zeringue, and D. J. Beebe, "Microenvironment design considerations for cellular scale studies," *Lab Chip*, vol. 4, no. 2, pp. 91–97, 2004.

[8] D. Juncker, H. Schmid, and E. Delamarche, "Multipurpose microfluidic probe," *Nature Materials*, vol. 4, no. 8, pp. 622–628, July 2005.

[9] M. A. Qasaimeh, S. G. Ricoult, and D. Juncker, "Microfluidic probes for use in life sciences and medicine," *Lab Chip*, vol. 13, no. 1, pp. 40–50, 2013.

[10] M. Safavieh, M. A. Qasaimeh, A. Vakil, D. Juncker, and T. Gervais, "Two-aperture microfluidic probes as flow dipoles: Theory and applications," *Scientific Rep.*, vol. 5, p. 11,943, July 2015.

[11] D. Chen, W. Dua, Y. Liua, W. Liua, A. Kuznetsovb, F. E. Mendezb, L. H. Philipsonb, and R. F. Ismagilova, "The chemistrode: A droplet-based microfluidic device for stimulation and recording with high temporal, spatial, and chemical resolution," *Proc. Nat. Acad. Sci.*, vol. 105, no. 44, pp. 16,843–16,848, Nov. 2008.

[12] G. V. Kaigala, R. D. Lovchik, and E. Delamarche, "Microfluidics in the 'open space' for performing localized chemistry on biological interfaces," *Angewandte Chemie Int. Edition*, vol. 51, no. 45, pp. 11,224–11,240, Nov. 2012.

[13] C. M. Perrault, M. A. Qasaimeh, and D. Juncker. (2009, June 4). The microfluidic probe: Operation and use for localized surface processing. *J. Visualized Experiments*. [Online]. 28, p. e1418. Available: https://www.jove.com/video/1418/the-microfluidic-probe-operation-use-for-localized-surface

[14] A. Queval, N. R. Ghattamaneni, C. M. Perrault, R. Gill, M. Mirzaei, R. A. McKinney, and D. Juncker, "Chamber and microfluidic probe for microperfusion of organotypic brain slices," *Lab Chip*, vol. 10, no. 3, pp. 326–334, 2010.

[15] G. V. Kaigala, R. D. Lovchik, U. Drechsler, and E. Delamarche, "A vertical microfluidic probe," *Langmuir*, vol. 27, no. 9, pp. 5686–5693, 2011.

[16] R. D. Lovchik, U. Drechsler, and E. Delamarche, "Multilayered microfluidic probe heads," *J. Micromechanics Microeng.*, vol. 19, no. 11, p. 11,5006, Sept. 2009.

[17] C. M. Perrault, M. A. Qasaimeh, T. Brastaviceanu, K. Anderson, Y. Kabakibo, and D. Juncker, "Integrated microfluidic probe station," *Rev. Sci. Instrum.*, vol. 81, no. 11, p. 11,5107, Nov. 2010.

[18] M. Hitzbleck, G. V. Kaigala, E. Delamarche, and R. D. Lovchik, "The floating microfluidic probe: Distance control between probe and sample using hydrodynamic levitation," *Appl. Phys. Lett.*, vol. 104, no. 26, p. 26,3501, 2014.

[19] M. A. Qasaimeh, T. Gervais, and D. Juncker, "Microfluidic quadrupole and floating concentration gradient," *Nature Commun.*, vol. 2, no. 464, 2011.

[20] C. W. Macosko, M. A. Ocansey, and H. H. Winter, "Steady planar extensions with lubricated dies," *J. Non-Newtonian Fluid Mechanics*, vol. 11, no. 3–4, pp. 301–316, 1982.

[21] M. Tanyeri, M. Ranka, N. Sittipolkula, and C. M. Schroeder, "A microfluidic-based hydrodynamic trap: Design and implementation," *Lab Chip*, vol. 11, no. 10, pp. 1786–1794, 2011.

[22] M. A. Qasaimeh, S. G. Ricoult, and D. Juncker, "Microfluidic probes to process surfaces, cells, and tissues," in *Selected Topics in Nanomedicine*, vol. 3, T. M. S. Chang, Ed. Singapore: World Scientific, 2014.

[23] D. Liazoghli, A. D. Roth, P. Thostrup, and D. R. Colman, "Substrate micropatterning as a new in vitro cell culture system to study myelination," *ACS Chem. Neurosci.*, vol. 3, no. 2, pp. 90–95, 2012.

[24] D. Stellwagen and R. C. Malenka, "Synaptic scaling mediated by glial TNF-α," *Nature*, vol. 440, no. 7087, pp. 1054–1059, Apr. 2006.

[25] T. M. Pearce, J. A. Wilson, S. G. Oakes, S. Y. Chiu, and J. C. Williams, "Integrated microelectrode array and microfluidics for temperature clamp of sensory neurons in culture," *Lab Chip*, vol. 5, no. 1, pp. 97–101, 2005.

[26] U. F. Braschler, A. Iannone, C. Spenger, J. Streit, and H. R. Lüscher, "A modified roller tube technique for organotypic cocultures of embryonic rat spinal cord, sensory ganglia and skeletal muscle," *J. Neurosci. Methods*, vol. 29, no. 2, pp. 121–129, 1989.

[27] B. H. Gähwiler, S. M. Thompson, and D. Muller, "Preparation and maintenance of organotypic slice cultures of CNS tissue," *Current Protocols Neurosci.*, vol. 6, no. 11, pp. 6–11, May 2001.

[28] R. D. Lovchik, G. V. Kaigala, M. Georgiadis, and E. Delamarche, "Micro-immunohistochemistry using a microfluidic probe," *Lab Chip*, vol. 12, no. 6, pp. 1040–1043, 2012.

[29] D. J. Dabbs, *Diagnostic Immunohistochem.: Theranostic and Genomic Applications.* Philadelphia, PA: Elsevier Saunders, 2014.

[30] L. A. Sternberger, P. H. Hardy, J. J. Cuculis, and H. G. Meyer, "The unlabeled antibody enzyme method of immunohistochemistry preparation and properties of soluble antigen-antibody complex (horseradish peroxidase-antihorseradish peroxidase) and its use in identification of spirochetes," *J. Histochem. Cytochem.*, vol. 18, no. 5, pp. 315–333, May 1970.

[31] M. R. Emmert-Buck, R. F. Bonner, P. D. Smith, and R. F. Chuaqui, "Laser capture microdissection," *Science*, vol. 274, no. 5289, pp. 998–1001, Nov. 1996.

[32] R. F. Bonner, M. Emmert-Buck, K. Cole, T. Pohida, R. Chuaqui, S. Goldstein, and L. A. Liotta, "Laser capture microdissection: Molecular analysis of tissue," *Sci.*, vol. 278, no. 5342, pp. 1481–1483, Nov. 1997.

[33] S. R. Lakhani and A. Ashworth, "Microarray and histopathological analysis of tumours: The future and the past," *Nature Rev. Cancer*, vol. 1, no. 2, pp. 151–157, Nov. 2001.

[34] G. Sauter, R. Simon, and K. Hillan, "Tissue microarrays in drug discovery," *Nature Rev. Drug Discovery*, vol. 2, no. 12, pp. 962–972, Dec. 2003.

[35] J. S. Mohammed, H. H. Caicedo, C. P. Fall, and D. T. Eddington, "Microfluidic add-on for standard electrophysiology chambers," *Lab Chip*, vol. 8, no. 7, pp. 1048–1055, 2008.

[36] C. B. Moelans, R. A. De Weger, E. Van der Wall, and P. J. Van Diest, "Current technologies for HER2 testing in breast cancer," *Crit. Rev. Oncology/Hematology*, vol. 80, no. 3, pp. 380–392, Dec. 2011.

[37] H. Craighead, "Future lab-on-a-chip technologies for interrogating individual molecules," *Nature*, vol. 442, pp. 387–393, July 2006.

[38] D. Falconnet, G. Csucs, H. M. Grandin, and M. Textor, "Surface engineering approaches to micropattern surfaces for cell-based assays," *Biomaterials*, vol. 27, no. 16, pp. 3044–3043-63, 2006.

[39] J. T. Delaney, P. J. Smith, and U. S. Schubert, "Inkjet printing of proteins," *Soft Matter*, vol. 5, no. 24, pp. 4866–4877, 2009.

[40] S. A. Ruiz and C. S. Chen, "Microcontact printing: A tool to pattern," *Soft Matter*, vol. 3, no. 2, pp. 168–177, 2007.

[41] J. Autebert, A. Kashyap, R. D. Lovchik, E. Delamarche, and G. V. Kaigala, "Hierarchical hydrodynamic flow confinement: Efficient use and retrieval of chemicals for microscale chemistry on surfaces," *Langmuir*, vol. 30, no. 12, pp. 3640–3645, 2014.

[42] M. A. Qasaimeh, R. Safavieh, and D. Juncker, "The generation of biochemical gradients in a microfluidic stagnant zone," in *Proc. 5th Int. Conf. Microtechnologies Medicine Biotechnology*, Quebec, Canada, 2009, pp. 62–63.

[43] K. R. King, S. Wang, A. Jayaraman, M. L. Yarmush, and M. Toner, "Microfluidic flow-encoded switching for parallel control of dynamic cellular microenvironments," *Lab Chip*, vol. 8, no. 1, pp. 107–116, 2008.

[44] S. Takayama, E. Ostuni, P. LeDuc, K. Naruse, D. E. Ingber, and G. M. Whitesides, "Selective chemical treatment of cellular microdomains using multiple laminar streams," *Chem. Biol.*, vol. 10, no. 2, pp. 123–130, Feb. 2003.

[45] H. Ali, R. M. Richardson, B. Haribabu, and R. Snyderman, "Chemoattractant receptor cross-desensitization," *J. Biological Chem.*, vol. 274, no. 10, pp. 6027–6030, Mar. 1999.

[46] E. D. Tomhave, R. M. Richardson, J. R. Didsbury, L. Menard, R. Snyderman, and H. Ali, "Cross-desensitization of receptors for peptide chemoattractants: Characterization of a new form of leukocyte regulation," *J. Immunology*, vol. 153, no. 7, pp. 3267–3275, Oct. 1994.

[47] M. Zimmermann, S. Bentley, H. Schmid, P. Hunziker, and E. Delamarche, "Continuous flow in open microfluidics using controlled evaporation," *Lab Chip*, vol. 5, no. 12, pp. 1355–1359, 2005.

[48] K. Khare, J. Zhou, and S. Yang, "Tunable open-channel microfluidics on soft poly (dimethylsiloxane) (PDMS) substrates with sinusoidal grooves," *Langmuir*, vol. 25, no. 21, pp. 12,794–12,799, 2009.

[49] N. M. Oliveira, A. I. Neto, W. Song, and J. F. Mano, "Two-dimensional open microfluidic devices by tuning the wettability on patterned superhydrophobic polymeric surface," *Appl. Phys. Express*, vol. 3, no. 8, p. 085,205, Aug. 2010.

[50] P. Dak, A. Ebrahimi, V. Swaminathan, C. Duarte-Guevara, R. Bashir, and M. A. Alam, "Droplet-based biosensing for lab-on-a-chip, open microfluidics platforms," *Biosensors*, vol. 6, no. 2, p. 14, Apr. 2016.

[51] M. M. Hamedi, B. Ünal, E. Kerr, A. C. Glavan, M. T. Fernandez-Abedulc, and G. M. Whitesides, "Coated and uncoated cellophane as materials for microplates and open-channel microfluidics devices," *Lab Chip*, vol. 16, no. 20, pp. 3885–3897, 2016.

[52] T. E. de Groot, K. S. Veserat, E. Berthier, D. J. Beebe, and A. B. Theberge, "Surface-tension driven open microfluidic platform for hanging droplet culture," *Lab Chip*, vol. 16, no. 2, pp. 334–344, 2016.

[53] A. Ainla, G. D. Jeffries, R. Brune, O. Orwar, and A. Jesorka, "A multifunctional pipette," *Lab Chip*, vol. 12, no. 7, pp. 1255–1261, 2012.

[54] A. Ahemaiti, A. Ainla, G. D. Jeffries, H. Wigström, O. Orwar, A. Jesorka, and K. Jardemark, "A multifunctional pipette for localized drug administration to brain slices," *J. Neurosci. Methods*, vol. 219, no. 2, pp. 292–296, Oct. 2013.

[55] C. Y. Chen, T. Y. Chien, C. K. Lin, C. W. Lin, Y. Z. Weng, and D. T. H. Chang, "Predicting target DNA sequences of DNA-binding proteins based on unbound structures," *PloS One*, vol. 7, no. 2, p. e30446, Feb. 2012.

[56] D. S. Latchman, "Transcription factors: An overview," *Int. J. Biochem. Cell Biol.*, vol. 29, no. 12, pp. 1305–1312, Dec. 1997.

[57] P. J. Mitchell and R. Tijan, "Transcriptional regulation in mammalian cells by sequence-specific DNA binding proteins," *Science*, vol. 245, no. 4916, pp. 371–378, 1989.

[58] E. M. Johnson-Chavarria, U. Agrawal, M. Tanyeri, T. E. Kuhlman, and C. M. Schroeder, "Automated single cell microbioreactor for monitoring intracellular dynamics and cell growth in free solution," *Lab Chip*, vol. 14, no. 15, pp. 2688–2697, 2014.

[59] X. Li, C. M. Schroeder, and K. D. Dorfman, "Modeling the stretching of wormlike chains in the presence of excluded volume," *Soft Matter*, vol. 11, no. 29, pp. 5947–5954, 2015.

[60] F. Latinwo and C. M. Schroeder, "Determining elasticity from single polymer dynamics," *Soft Matter*, vol. 10, no. 13, pp. 2178–2187, 2014.

[61] M. Tanyeri and C. M. Schroeder, "Flow-based particle trapping and manipulation," in *Encyclopedia of Microfluidics and Nanofluidics.* New York: Springer, 2014, pp. 1–9.

[62] R. Dylla-Spears, J. E. Townsend, L. Jen-Jacobson, L. L. Sohn, and S. J. Muller, "Single-molecule sequence detection via microfluidic planar extensional flow at a stagnation point," *Lab Chip*, vol. 10, no. 12, pp. 1543–1549, 2010.

[63] M. A. Qasaimeh, M. Astolfi, M. Pyzik, S. Vidal, and D. Juncker, "Neutrophil dynamics during migration in microfluidic concentration gradients," in *Proc. 2014 40th Annu. Northeast Bioengineering Conf.*, Boston, MA, pp. 1–2.

[64] M. A. Qasaimeh, M. Astolfi, M. Pyzik, S. Vidal, and D. Juncker, "Neutrophils migrate longer distances in moving microfluidic concentration gradients compared to static ones," in *Proc. 17th Int. Conf. Miniaturized Systems Chemistry Life Sciences*, Freiburg, Germany, 2013, pp. 2007–2009.

[65] G. M. Whitesides, "The origins and future of microfluidics," *Nature*, vol. 442, pp. 368–373, July 2006.

[66] Y. T. Kim and R. Langer, "Microfluidics in nanomedicine," *Rev. Cell Biol. Molecular Medicine*, vol. 1, no. 2, pp. 127–152, July 2015.

N